PROBABILISTIC FACIES PREDICTION IN A CARBONATE GAS RESERVOIR OF IRAN USING STOCHASTIC SEISMIC INVERSION AND CONNECTIVITY ALGORITHM

HAMID REZA ANSARI[1], REZA MOTAFAKKERFARD[1] and MOHAMMAD ALI RIAHI[2]

[1] *Department of Petroleum Exploration Engineering, Abadan Faculty of Petroleum Engineering, Petroleum University of Technology, Abadan, Iran. ansari.hamid.r@gmail.com*
[2] *Institute of Geophysics, University of Tehran, Tehran, Iran.*

(Received December 18, 2013; revised version accepted November 18, 2014)

ABSTRACT

Ansari, H.R., Motafakkerfard, R. and Riahi, M.A., 2015. Probabilistic facies prediction in a carbonate gas reservoir of Iran using stochastic seismic inversion and connectivity algorithm. *Journal of Seismic Exploration*, 24: 15-35.

Inversion methods are valuable tools for obtaining reservoir properties from seismic data. However, results of the seismic inversion are band-limited due to band-limited source wavelet. Therefore, the low and high frequency information is lost in seismic traces. In order to overcome this problem, well logs and seismic data were used together in a seismic inversion algorithm using stochastic methods. In this paper, the stochastic inversion method was based on spectral simulation to create acoustic impedance realizations. Also, an initial broad-band model was derived from kriging of the well log data. Then, spectral simulation was applied for the seismic inversion. This method was conducted on one of the marine carbonate gas fields in Iran and the results were compared with deterministic inversion.

In the second part of this study, acoustic impedance realizations and rock density volume, obtained from the previous section, were combined with instantaneous frequency as the input of an unsupervised neural network for clustering the three rock facies and a vector quantizer network was utilized for this purpose. The network results were calibrated with porosity in the well location and provided threshold parameters to conduct the connectivity facies analysis. Finally, the connectivity algorithm was applied to all the realizations of stochastic inversion results to achieve highly probable favorable facies.

KEY WORDS: stochastic inversion, unsupervised neural network, probabilistic facies, connectivity algorithm.

0963-0651/15/$5.00

INTRODUCTION

Acoustic impedance (AI) is an important attribute obtained by virtue of the inversion of seismic data. There are many methods for seismic inversion and most of the available methods are based on minimizing differences between model and observed traces. These methods are commonly referred to as "deterministic inversion". The result of a deterministic inversion is the relatively smooth estimation of the impedance (Francis, 2006a). Due to the band-limitation of seismic traces caused by source wavelet, low and high frequencies are lost in the seismic data. Therefore, deterministic methods cannot reproduce the absolute values of the impedance observed in the wells. More details on the limitation of deterministic inversion can be found in Francis (2005; 2006a).

Stochastic (or geostatistical) inversion is an approach which is applied for overcoming the mentioned limitations of deterministic inversion. Another advantage of stochastic inversion is in computing a set of realizations used for appreciating the uncertainty in seismic inversion.

The geostatistical inversion method was presented by Bortoli et al. (1993) and Haas and Dubrule (1994) for the first time. This technique was a local trace by trace optimization method and incorporated sequential Gaussian simulation (Deutsch and Journel, 1998) to invert seismic data. Debeye et al. (1996) presented the same geostatistical inversion method by adding the simulated annealing optimization. Several studies have been conducted on geostatistical inversion (Kane et al., 1999; Buland and Omre, 2003; Eidsvik et al., 2004; Francis, 2006a; 2006b; Gonzalez et al., 2008).

Another method is global search technique for minimizing the mismatch between observed data and forward synthetic model. Francis (2006a; 2006b) exploited the fast Fourier transform based on spectral simulation in order to construct multi-impedance realization conditional to well log data. The advantage of the global methods such as spectral simulation is that they are faster than sequential simulation methods.

In this study, AI realizations obtained from stochastic inversion algorithm was based on spectral simulation method (Pardo-Iguzquiza and Chica-Olmo, 1993; Francis, 2006a; 2006b). This method was conducted in frequency domain using geostatistical simulation. Spectral simulation is a global method which uses a global density spectrum of variogram models and thus the inverse Fourier transform is performed only once to generate a realization.

The second part of this study was facies clustering using multi attributes analysis based on neural network clustering and connectivity algorithm (Deutsch, 1998). Facies term is used for categorical groups, not merely by lithology type, but also by the same property or a set of properties (Bosch et al.,

2010). The intelligent seismic facies analysis would be supervised by the priori geological information or could be unsupervised when there is not enough data for guiding the analysis (Matos et al., 2005). An unsupervised vector quantization (Gersho and Gray, 1992) was trained and utilized for clustering in this study. Unsupervised neural networks do not require any target dataset. Instead, they try to find patterns/clusters within the input dataset in multi-dimensional space (Russel, 2005). The results of neural network were applied to obtain the threshold parameter in the connectivity algorithm in order to construct probability facies cube.

Geological and data overview

The area of study was an Iranian gas field located in the Persian Gulf. Several reservoirs were explored and found to be productive in this field. The oil reservoir belonged to the Khami and Bangestan group formations and the gas-bearing formations were the Kangan and Dalan formations of Triassic and Permian age. The field consisted of four independent reservoir layers which were K_1, K_2, K_3 and K_4 from top to bottom. These units were mainly composed of dolomite, limestone, and some streak anhydrite. K_2 and K_4 constituted major gas reservoirs (Tavakoli et al., 2011). A massive anhydrite body (the Nar member) separated K_4 from the underlying K_5 unit which had poor reservoir qualities (Fig. 1).

Available data for this study were 3D post-stack seismic section operated to cover 370 km^2 and AI logs prepared from four wells. Three wells (B, C, D) were used directly in stochastic inversion process and another well (A) was used for validating the results. Well data consisted of both a set of conventional well logs and petrophysical measurements such as resistivity, porosity, and density. The litho-stratigraphic charts of wells A and C, obtained from cutting data, were prepared in the mentioned data set. Additionally, three interpreted horizon surfaces, introduced as Dashtak-S_7, K_1 and K_4, were used for modeling.

METHODS

A priori model building

Fig. 2 shows the general scheme of methodology workflow. The initial step is the preparation of data, such as picking time horizons, extracting wavelet, producing AI log from the sonic and density logs, and getting spatial relationships. In order to describe the spatial relationships, the semi-variogram is most commonly applied in geostatistical methods. Semi-variogram is half of the variogram that is defined as half of the variance of the difference between the two values located l distance apart (Kelkar and Perez, 2002). In a large

distance, the semi-variogram reaches a value called *sill* and the distance at which the semi-variogram reaches sill is called *range*. Then, estimated variograms fit a common *variogram model* such as exponential, spherical, or Gaussian.

In the next step, a 3D broad-band model is created using picked horizons and interpolating well log by kriging. The kriging method utilizes a linear estimation procedure in order to estimate a value in an unsampled location. All kriging methods are elaborations on the basic generalized linear regression algorithm. Let the value estimation be conducted in an unsampled location $Z^*(\mathbf{u}_i)$ from the values of n-point neighboring location $Z(\mathbf{u}_i)$, i = 1, 2... n. Then, the simple kriging estimator is defined by Deutsch and Journel (1992):

$$Z^*(\mathbf{u}_i) = \sum_{i=1}^{n} \lambda_i Z^*(\mathbf{u}_i) + (1 - \sum_{i=1}^{n} \lambda_i)m \quad , \tag{1}$$

where λ_i is the weight assigned to the neighboring value and m is the expected value of Z(u). Weights are estimated by solving the kriging system depending on the spatial relationship between the neighboring observations.

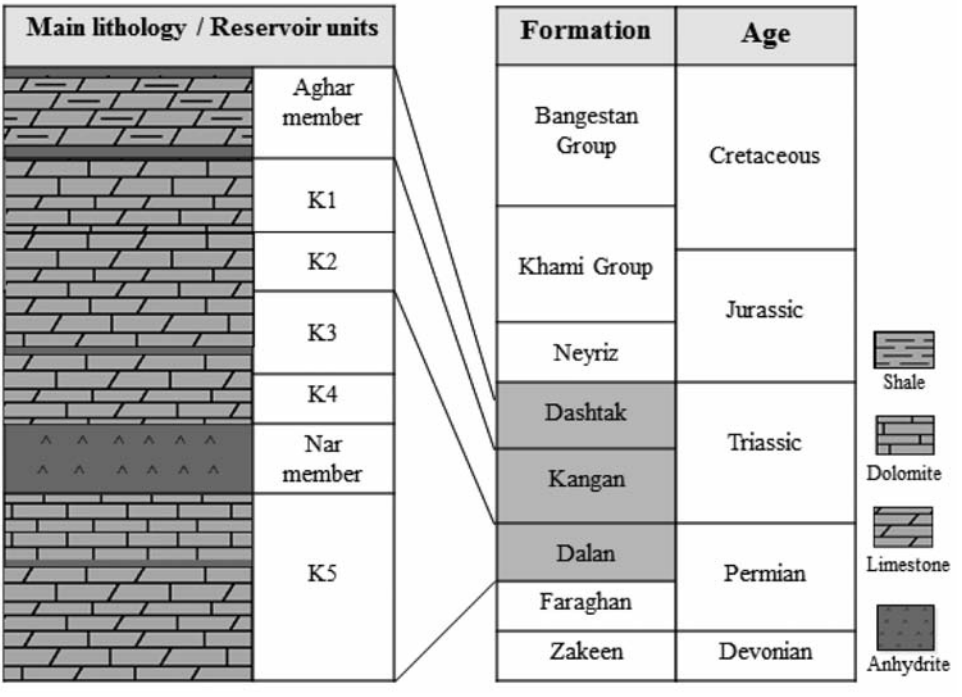

Fig. 1. Generalized stratigraphic chart of this study field (not to scale). The lower Dashtak, Kangan and upper Dalan were used in this study.

In addition to the estimate in the least square scenes, kriging has another advantage. It also assigns the uncertainty to the estimate at any unsampled location. The uncertainty is small and close to sampled locations and will increase away from them. Finally, the 3D model is created by kriging interpolation and applied as a priori model in both deterministic and stochastic inversion.

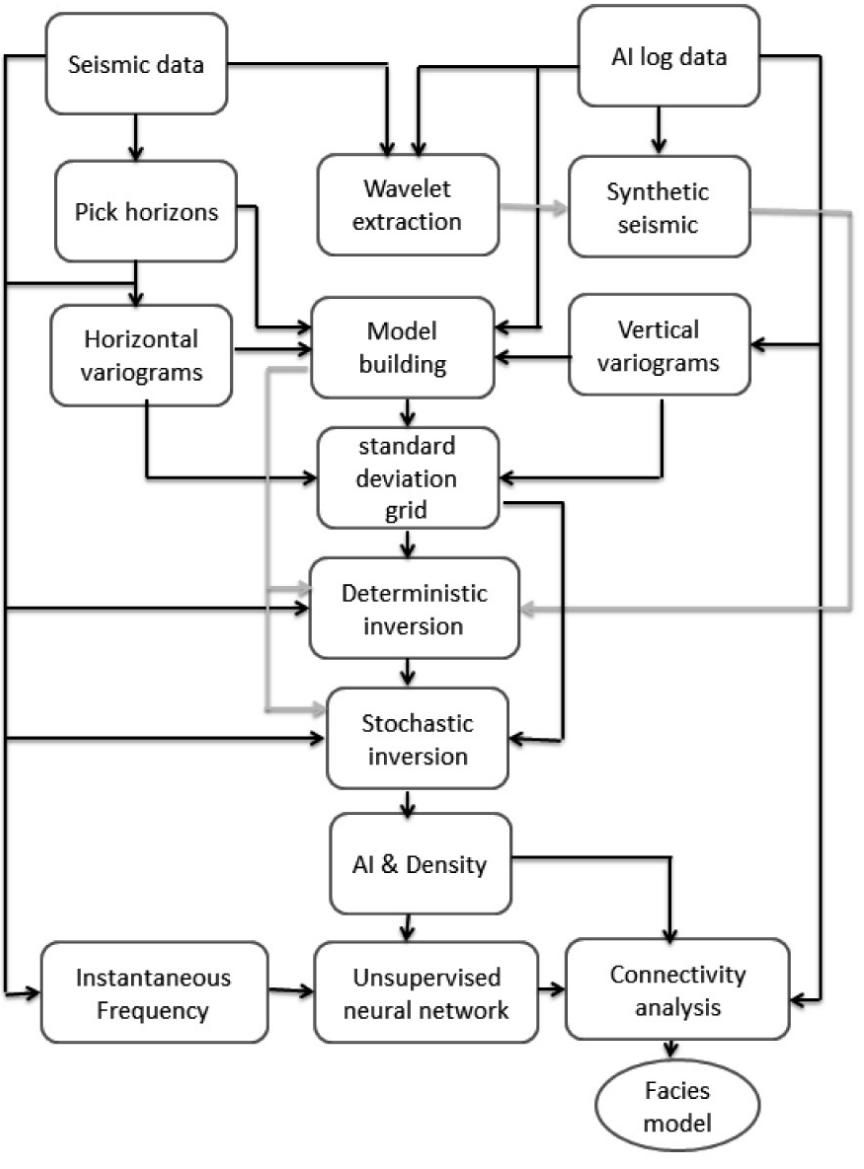

Fig. 2. General workflow of this study. The main process was stochastic inversion and final result was probability facies model.

Deterministic inversion

The observed data, **d**, and the model parameter, **m**, can be generally related through a function, G, in the following forward model:

$$\mathbf{d} = G(\mathbf{m}) + \mathbf{e} \quad , \tag{2}$$

where **e** is the error vector. The purpose of the inverse problem theory is the estimation of **m**. In the seismic scenes, the signals recorded at the surface are data observation and **m** which is referred to as earth model. Also, the forward model is described by convolution model:

$$s(t) = r(t) * w(t) + n(t) \quad . \tag{3}$$

s(t) represents the seismic traces indicated by the convolution of reflectivity, r(t), and wavelet, w(t), plus random noise, n(t). Reflectivity is related to the acoustic impedance as follows:

$$r(t) = [AI(t+1) - AI(t)]/[AI(t+1) + AI(t)] \quad . \tag{4}$$

Let:

$$g(AI,t) = \{[AI(t+1) - AI(t)]/[AI(t+1) + AI(t)]\} * w(t) \quad . \tag{5}$$

Then:

$$s(t) = g(AI,t) + n(t) \quad . \tag{6}$$

Eqs. (5) and (6) represent nonlinear inversion for the AI. Deterministic methods use an approximation method for linearization. The Taylor series approximation can be applied for linearization:

$$g(AI,t) \approx g(AI_0,t) + \partial g(AI,t)/\partial AI\big|_{AI=AI_0} \Delta AI \quad , \tag{7}$$

where AI_0 is the initial acoustic impedance and ΔAI is the change in AI. Suppose the vector $s_0(t)$ such that:

$$s_0(t) = g(AI_0,t) \quad , \tag{8}$$

and

$$G = \partial g(AI,t)/\partial AI\big|_{AI=AI_0} \quad . \tag{9}$$

Then, if we substitute them in eq. (6), we can summarize as:

$$s(t) - s_0(t) = \Delta s(t) = G\,\Delta AI + n(t) \quad . \tag{10}$$

Eq. (10) is the explicit linear forward model explained in the pose of Eq. (2). This problem is an over-determined problem and the least squares error method is used to solve the equation.

In this study, deterministic inversion was seismic model-based inversion that uses the generalized linear inversion (GLI) method (Cooke and Schneider, 1983) to obtain an optimal impedance solution whose forward convolution sounds to be suitable for the seismic in a least squares sense (Russel, 1988).

Stochastic inversion

Stochastic (geostatistical) inversion adds well log data using spatial relationships in stochastic processes scenes. In this study, stochastic inversion exploited the FFT-based spectral simulation method to generate impedance realizations, conditional to the well impedance data (Francis, 2006b). Details of the 3D frequency domain simulation, which is called Fourier integral method, were discussed in Pardo-Iguzquiza and Chica-Olmo (1993). Briefly, the covariance function is determined for each layer using a 3D anisotropic variogram and is characterized by a density spectrum in frequency domain. Consider C(h) as a discrete covariance function; then, the discrete spectral density $S(\omega)$ is the Fourier transform of C(h). The spectral simulation can be summarized as follows:

1. Computing covariance (or variogram) functions in each layer.

2. Calculating $S(\omega)$ from C(h) using the (fast) Fourier transform.

3. Calculating the amplitude spectrum from $S(\omega)$. The square root of spectral density is amplitude spectrum.

4. Generating a random phase spectrum. The amplitude and phase spectrum are the Fourier transform parameters of a real random field.

5. Using inverse (fast) Fourier transform of amplitude and phase spectrum to obtain the real random field variables.

The amplitude spectrum can be honored globally over the whole field, instead of only within searching the neighborhoods, as with the traditional SGS method (Yao et al., 2004). The spectral density is calculated once from covariance function and inverse (fast) Fourier transform is accomplished on the amplitude and phase spectrum only once to construct realization. Thereby, this method is fast, especially when FFT is used. Increasing the speed of algorithm causes a decrease in the computational cost.

Finally, stochastic inversion based on FFT-spectral simulation can be achieved as follows:

1. Building initial model using kriging of well log data between seismic

horizons.

2. Providing a spatial well constraint based on standard deviation map obtained from simple kriging of the well data. Standard deviation is zero in well locations and reaches the maximum value away from the well locations, at distances greater than the variogram ranges. This map is applied to relative importance of seismic data in inversion process. Therefore, when far from the well locations, seismic data are significant for model construction.

3. The AI values in well locations are converted to a standard Gaussian PDF.

4. Inverting seismic data in the stochastic framework in frequency domain. Conditioning to seismic data is accomplished by exploiting the GLI to update the initial geostatistical realizations of AI. In spectral simulation, separation of amplitude and phase allow for updating the model with other information. Therefore, missing frequencies can be simulated by a priori well log model.

5. In the final step, stochastic inversion results must be back transformed from their standard Gaussian PDF into original impedance unit, which is obtained by using the inverse normal score transform.

Unsupervised neural networks

In the unsupervised neural networks, the weights and biases are learned in response to network inputs only. They classify the input data into a finite number of clusters. Vector-quantization (VQ) networks (Gersho and Gray, 1992) are a form of unsupervised Kohonen neural networks. A VQ network has only one hidden layer of nodes, where each node corresponds to one potential cluster. This network consists of a number of codebook vectors, which constitute cluster centers. When a new case is learned, the locations of the codebook vectors are adapted so that the mean Euclidian distance between each data point is minimized and is the closest to the codebook vector. This algorithm is called competitive learning; i.e., the neurons in outputs compete with each other for the inputs.

In this study, three attributes were used as input to the VQ neural network including AI realization, rock density, and instantaneous frequency. AI realizations were the results of stochastic inversion. The rock density volume can be obtained using linear regression of the average of all realizations. The instantaneous frequency can be obtained from original seismic volume. The output was a unique volume of facies classes.

Connectivity algorithm

The neural network results are calibrated by well data and then the threshold impedances of the facies are obtained. The connectivity algorithm scans each realization. If the grid nodes are within the specified AI range, they are considered net connected; otherwise, they are non-net. The output of this analysis can be represented as probability cube obtained from the probability of the grid nodes to be connected given a specified range (Deutsch, 1998). Fig. 3 shows a schematic diagram of constructing probabilistic facies model using connectivity algorithm.

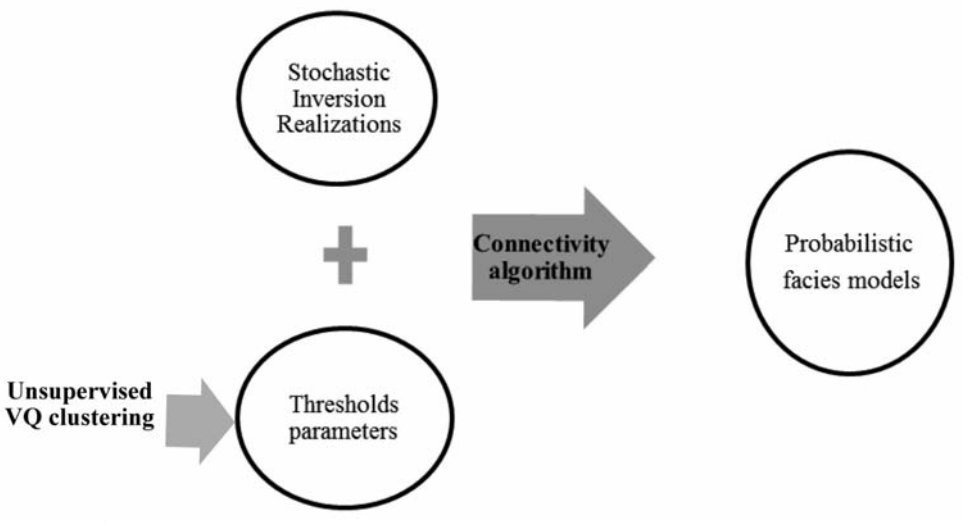

Fig. 3. Schematic diagram of constructing the probabilistic facies model using connectivity algorithm.

CASE STUDY

AI stochastic inversion

Variogram parameters such as range, sill, and model are essential for the construction of the prior AI model. To obtain variogram parameters, it is necessary to consider stationarity assumption in the variogram analysis of data. Stationarity implies that data must be trendless. Relative impedance data does not contain trend. Seismic colored inversion (Lancaster and Whitcombe, 2000) is a tool that converts the seismic data into relative impedance data. In simple terms, colored inversion defines an operator by the analysis of seismic and well log data. The operator of colored inversion transforms the average seismic trace spectra into the desired average AI log spectrum.

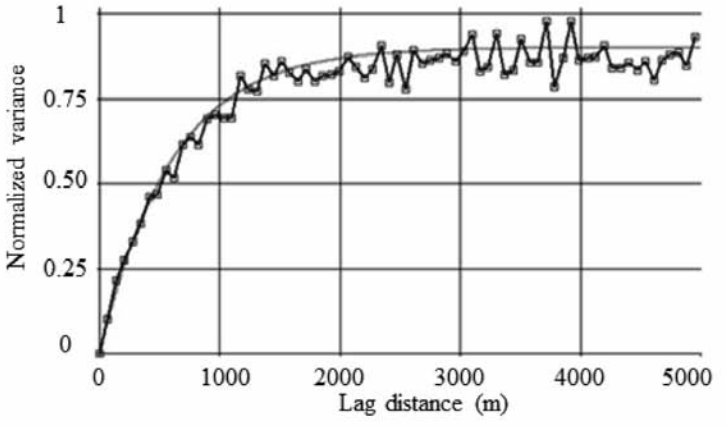

a)

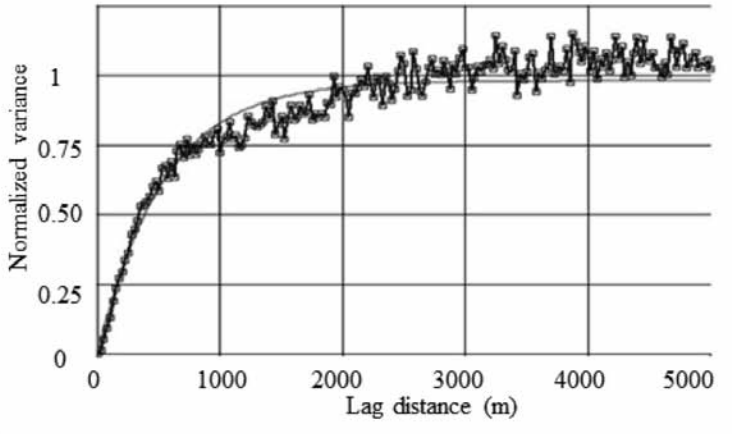

b)

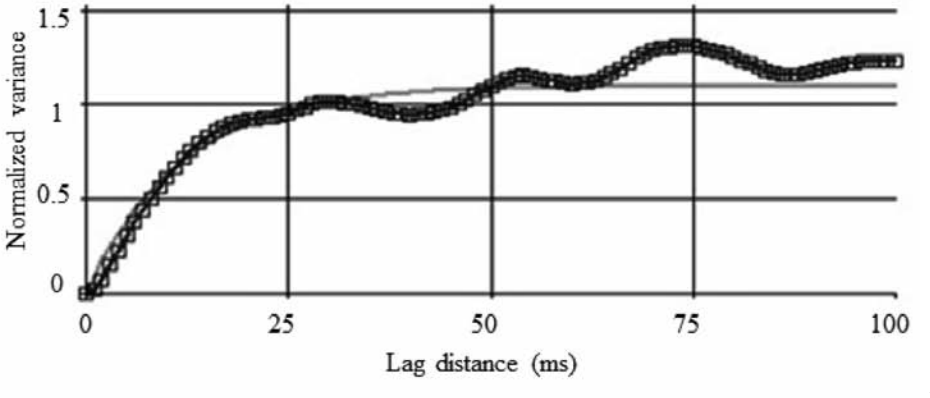

c)

Fig. 4. Variograms estimated for zone 2 in a) inline direction, b) cross-line direction, and c) vertical direction.

Horizontal variograms were obtained from SCI results and vertical variograms were acquired from log data (Fig. 4). Exponential models were the best fitting model to the variogram results. In the next step, some zones must be defined for constructing the initial 3D model. For this purpose, three horizons were applied to define four zones. Each zone was bounded by two horizons or by a horizon and top/base of the model. Then, a simple kriging method was used to interpolate the AI values between the zones in order to build initial 3D model. Moreover, a standard deviation map was computed according to the initial models. The standard deviation map is also called error grid map. The error grid map was zero in the well locations and reached a maximum value at distances greater than variogram range. The error grid was used to control the inversion convergence criteria.

Before conducting any inversion process, a wavelet was extracted from seismic data by statistical method. Fig. 5 represents the extracted wavelet in time domain, where the correlation between synthetic and real seismic in the well locations was average 0.74. In addition to seismic and wavelet, the initial model containing low frequency and error grid was considered to be the inputs for inversion algorithm. Inversion output was assessed according to cross validation and quality check (QC) in the well locations. Well A, in turn, was hidden and the three remaining wells were used in the model building. QC between well A and the inversion result is displayed in Fig. 6. In addition to QC, the inversion results monitored the existing quantity by root mean square

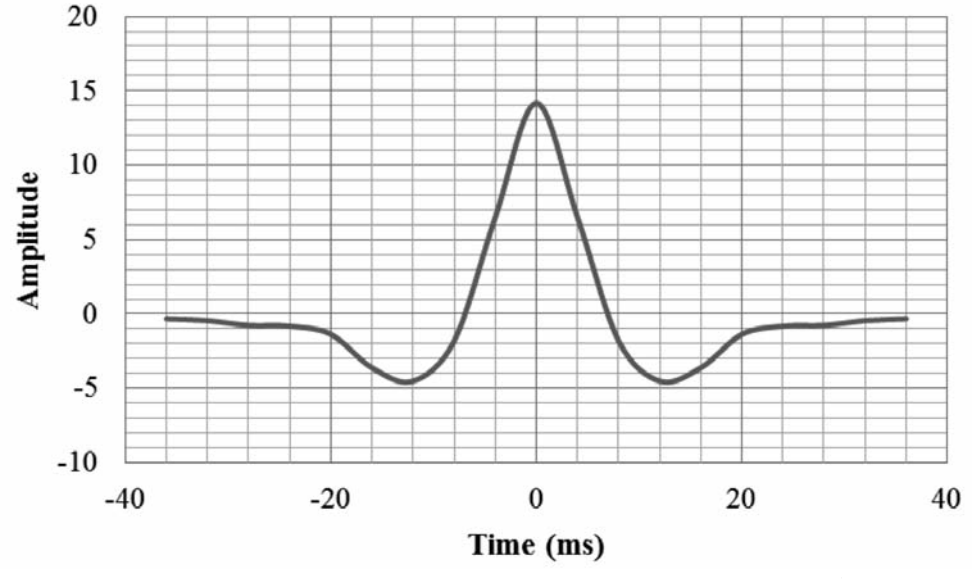

Fig. 5. Wavelet extracted from seismic data using statistical method. Cross correlation between synthetic and real seismic in well locations was average 0.74.

(RMS). The RMS results showed that the synthetic seismic error had the RMS amplitude of less than 10% of the RMS of the seismic section, which was acceptable for the seismic inversion. The synthetic seismic error referred to the difference between synthetic and seismic traces. The synthetic section was produced by eq. (5).

Correlation coefficient (R) between the deterministic inversion and real AI log in the hidden well was 0.79, while this value for the stochastic method was 0.82. Fig 7 shows the cumulative distribution (CDF) plots for the error of each model. In this figure, the error was defined by the difference between predicted results and well log data. Details of probability distribution of the errors are gathered in Table 1. According to Table 1 and Fig. 7, 52.77% of the stochastic estimations had the error of less than 1000 m/s $*$ g/cm^3, while this value was 47.99% for the deterministic inversion. If there was the range of 15000 m/s $*$ g/cm^3 for the AI values and the difference between actual and prediction was 1000 m/s $*$ g/cm^3, then the error would be 6.7%. A deep insight into the above results reveals that R increased and error decreased in the stochastic method. It can be clearly understood that the stochastic method had better performance than the deterministic method.

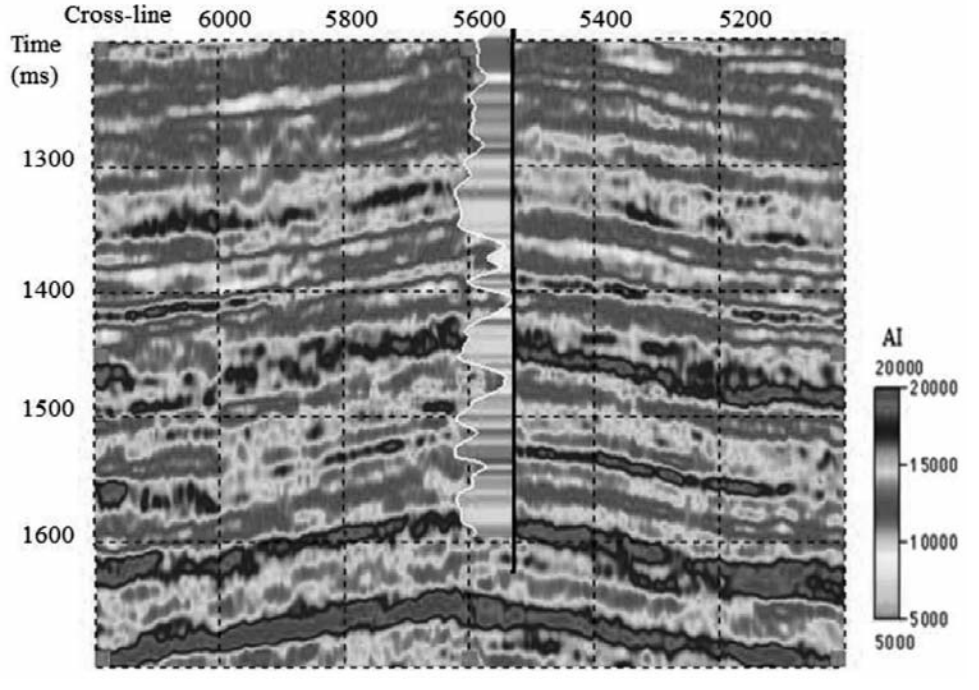

Fig. 6. QC between hidden well A and seismic inversion result in the acoustic impedance domain (m/s $*$ g/cm^3). Low frequency component of the log is not present in deterministic inversion.

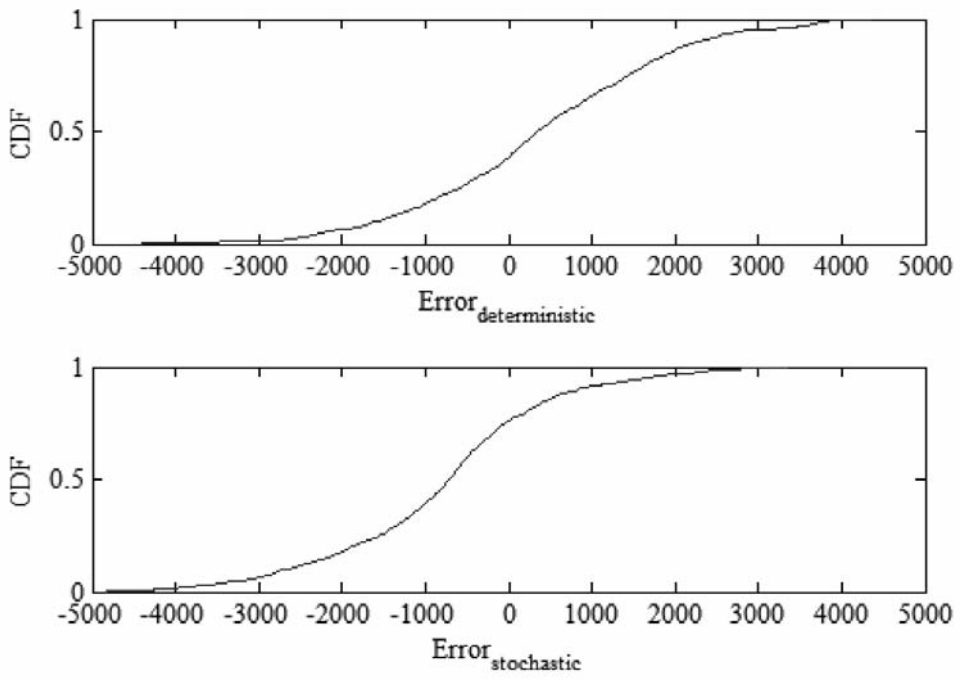

Fig. 7. CDF plots of error for deterministic and stochastic methods.

Table 1. Probability distribution of the inversion errors. The table shows that more than 50% of stochastic results have an error less than 1000 m/s $*$ g/cm^3.

Method	$\|e\| < 500$	$\|e\| < 1000$	$\|e\| < 1500$	$\|e\| < 2000$
Deterministic	0.2604	0.4799	0.6530	0.7902
Stochastic	0.27294	0.5277	0.6856	0.7985

Low frequency components were added to the AI model using the stochastic inversion. All the previous steps were applied as input to the current step as illustrated graphically in Fig. 2. Fig. 8 demonstrates a realization of the final stochastic result. Fig. 9 represents both the deterministic and stochastic results where a low pass frequency filter was done to them. The comparison between the deterministic and stochastic inversion represented that the deterministic method was unable to reproduce the full range of impedance as their result and deterministic impedance was smoother than a stochastic one.

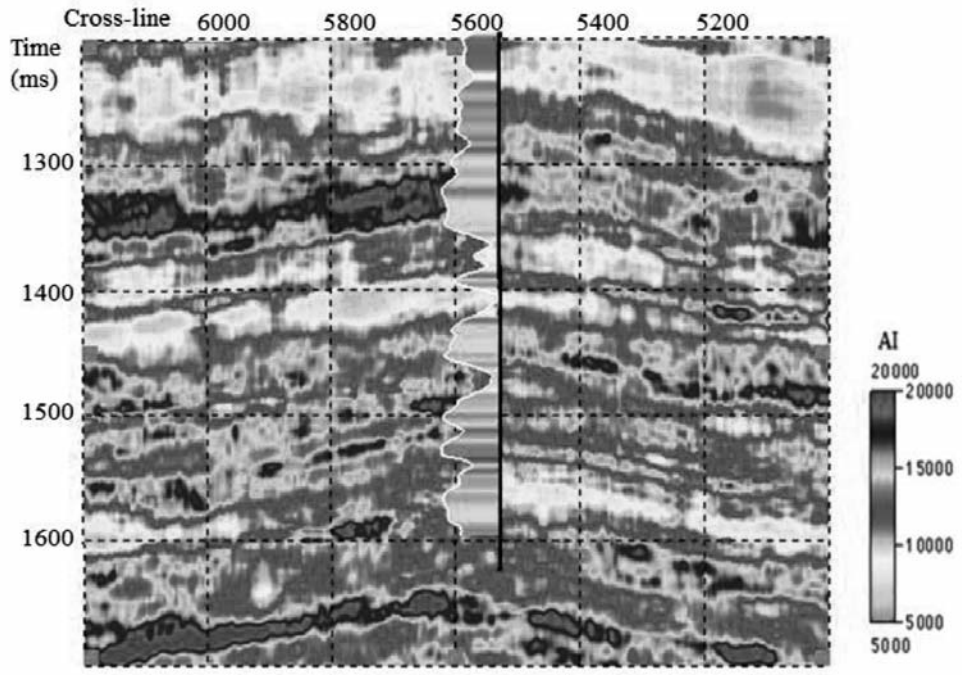

Fig. 8. QC between hidden well A and a realization of stochastic inversion result.

All realizations can be summarized in one section by averaging them (Fig. 10). The mean was much smoother than the realization displayed before and appeared slightly similar to the deterministic inversion results; however, the stochastic method improved the deterministic results. Fig. 11 indicates that the standard deviation of all realizations had larger variability near the bottom of the model due to the slight well constraint at the bottom of the model.

Facies estimation

Facies estimation is an important step for reservoir characterization. Estimating the facies by indirect method, with seismic attributes and log data, is customary in petroleum industries. For this purpose, multi realization AI, density, and instantaneous frequency were used in this step. Instantaneous frequency responds to both wave propagation effects and depositional characteristics and has high frequency in thin bed zones (Taner et al., 1994).

An unsupervised neural network is a good tool for facies clustering when there is not enough data for the modeling process. Instantaneous frequency, density, and five AI realizations from the previous section were used as input

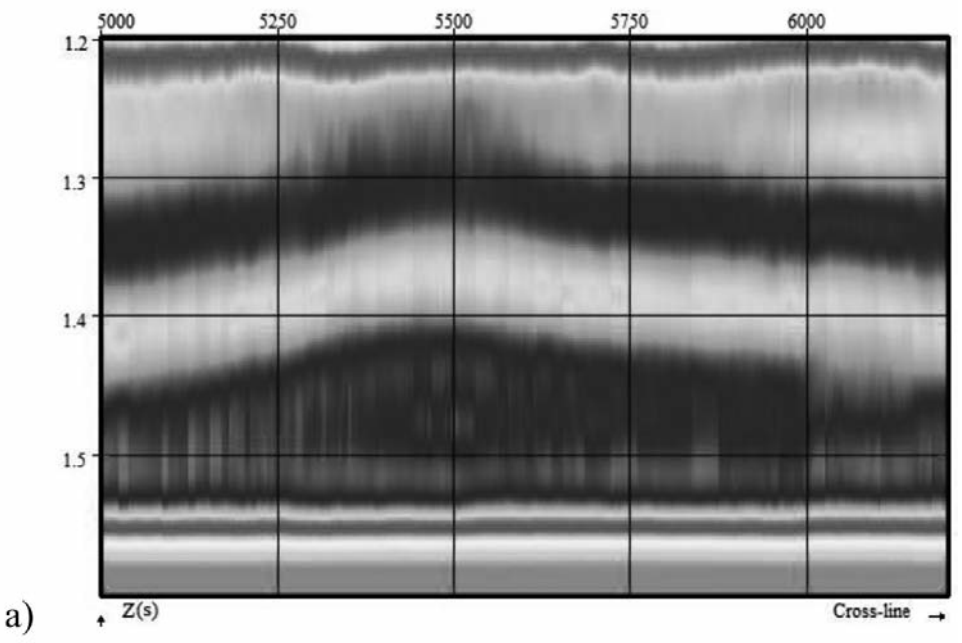

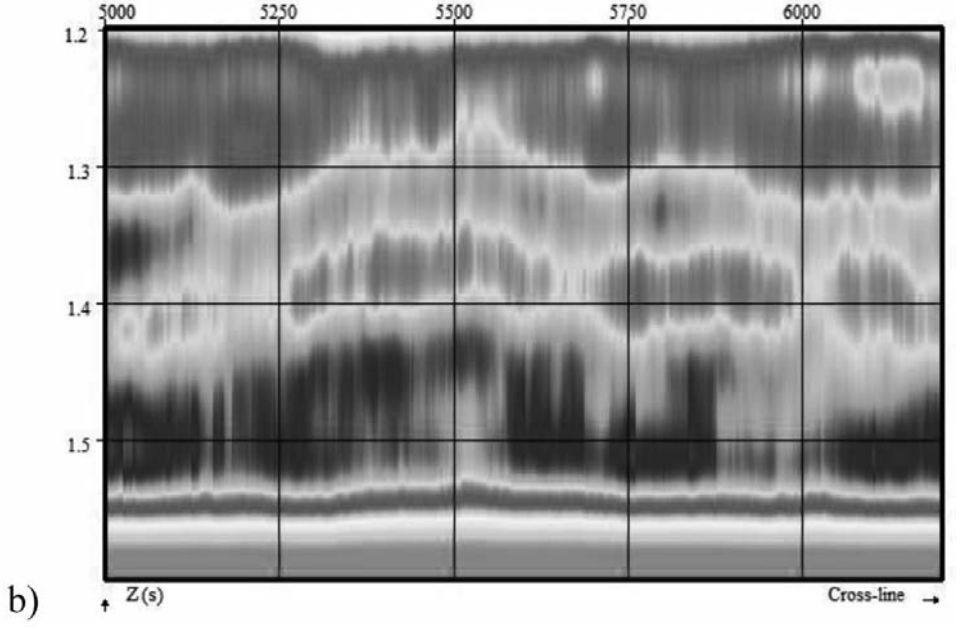

Fig. 9. Low frequency pass filter (below 10 Hz) was performed on: a) the deterministic inversion, and b) the mean of the stochastic realizations. It is clear that low frequency components were missed in deterministic section.

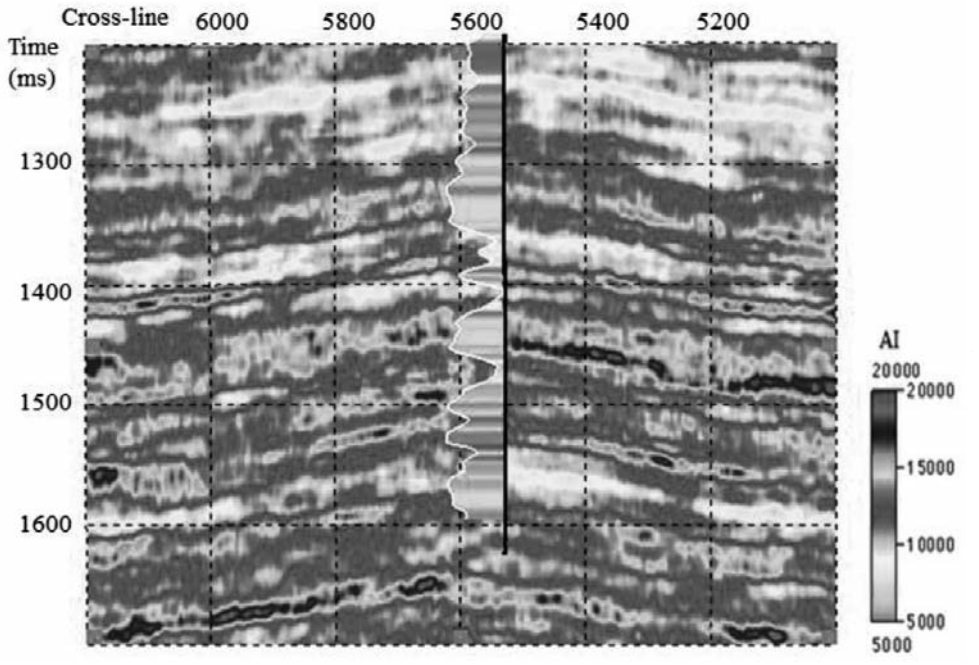

Fig. 10. Mean of the stochastic realizations.

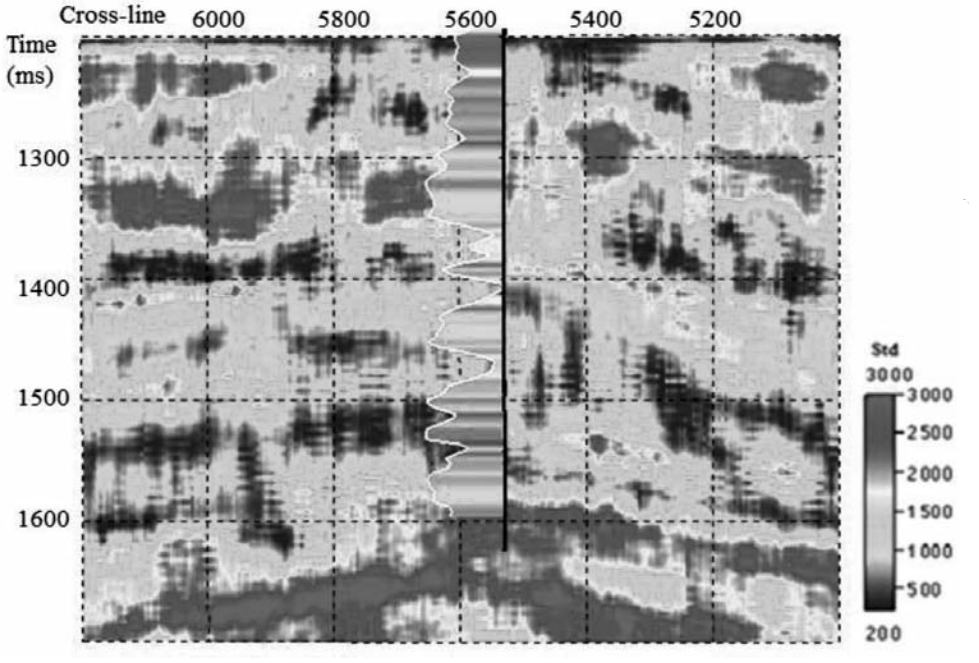

Fig. 11. Standard deviation of all realizations in the AI domain (m/s $*$ g/cm^3). Variability at bottom model increased.

for training the unsupervised VQ network to create three clusters. 488 vectors were used to cluster class 1 and average match was 0.91607. Class 2 was trained by 736 vectors and 0.907354 matching. 473 vectors by 0.895914 matching were used for the final class. Fig. 12 illustrates a crossplot of the extracted porosity from the log values against AI values in the well locations; the color codes were assigned to the network classification. There were three types of the facies that can be clearly distinguished from it. Number one indicated facies with high AI and very low porosity. Cluster center of density nodes was 2.85 (between dolomite and anhydrite density) and was called unfavorable zone. Perhaps, poor reservoir properties in this zone can be due to the existence of anhydrite which should be checked in a complementary study. Facies 3 was a favorable zone with higher porosity and facies 2 was intermediate between facies 1 and 3. Cluster centers of the facies are presented in Table 2. The density decreased in the facies 3 due to the existence of gas in the reservoir zone. The facies classification and their comparison with actual data are shown in Fig. 13 in two well locations. The actual data revealed that the dominant lithology of code 1 was anhydrite. Dolomite and limestone were the dominant lithologies in codes 2 and 3, respectively. The results revealed that favorable facies mainly consisted of limestone and facies 1 was poor reservoir because of containing anhydrite.

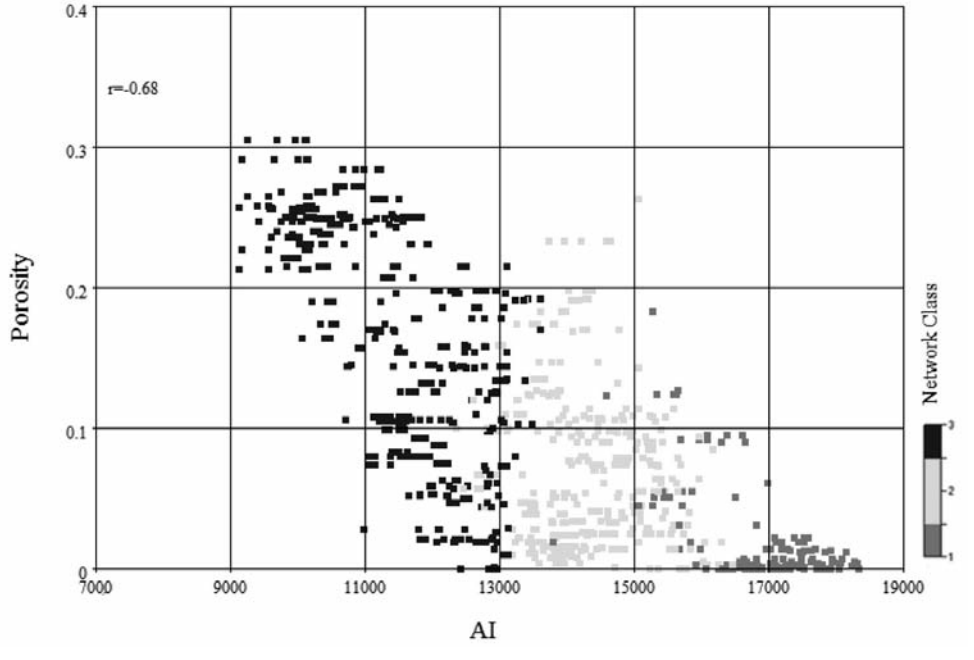

Fig. 12. Crossplot of the porosity against acoustic impedance from the mean of realizations values in well C location; the color scale is assigned to the network classification (AI and porosity were m/s * g/cm^3 and v/v, respectively).

Table 2. Centers of network clusters is tabled for some input node. Facies 1 is thin unfavorable beds and facies 3 is favorable massive beds (AI realizations are m/s $*$ g/cm^3 and density is g/cm^3).

Node \ Class	Center 1	Center 2	Center 3
AI Realization 1	16836.316	14258.045	12223.82
AI Realization 2	17182.964	14561.502	12159.55
AI Realization 3	16628.597	13975.793	11105.78
AI Realization 4	16916.472	14606.673	12385.96
AI Realization 5	16762.242	14178.476	11049.69
Density	2.852837	2.692746	2.533791

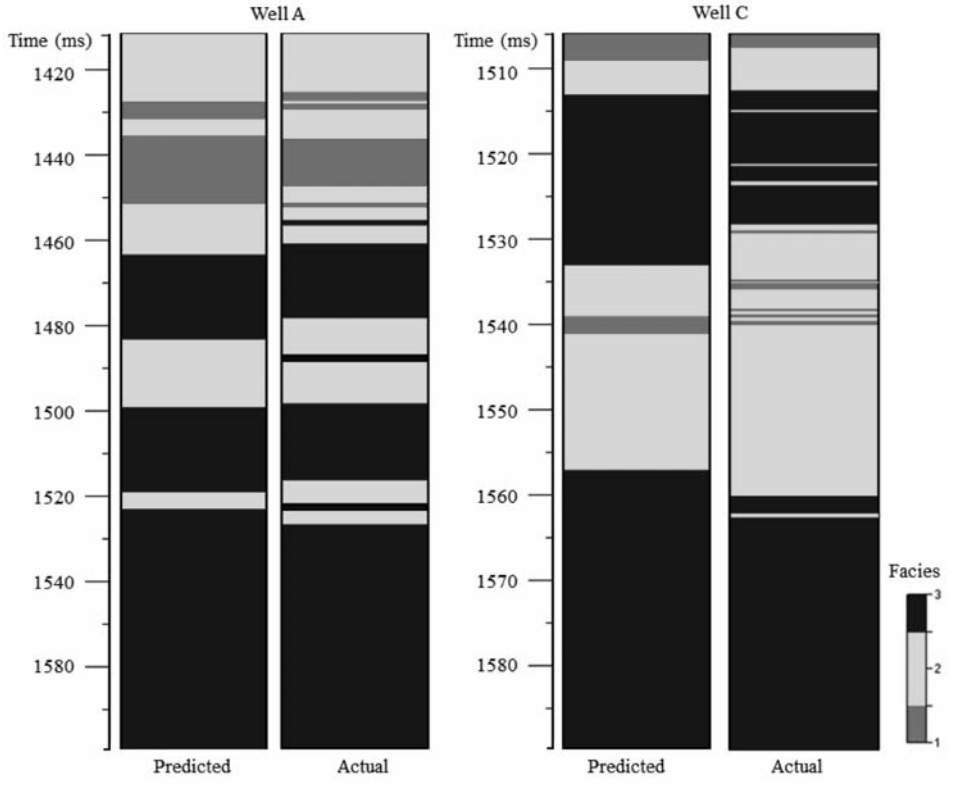

Fig. 13. Actual and predicted facies at well A and C. Actual classification was based on cutting data and predicted chart was gathered by unsupervised VQ.

Briefly speaking, an AI higher than 16000 (m/s $*$ g/cm^3) indicated facies 1, lower than 13000 indicated facies 3, and between them showed facies 2. With this cut off range, reservoir connectivity analysis was done based on facies models. Fig. 14 shows that facies 1 was a thinner bed and facies 3 was massive facies with more than 0.8 probabilities.

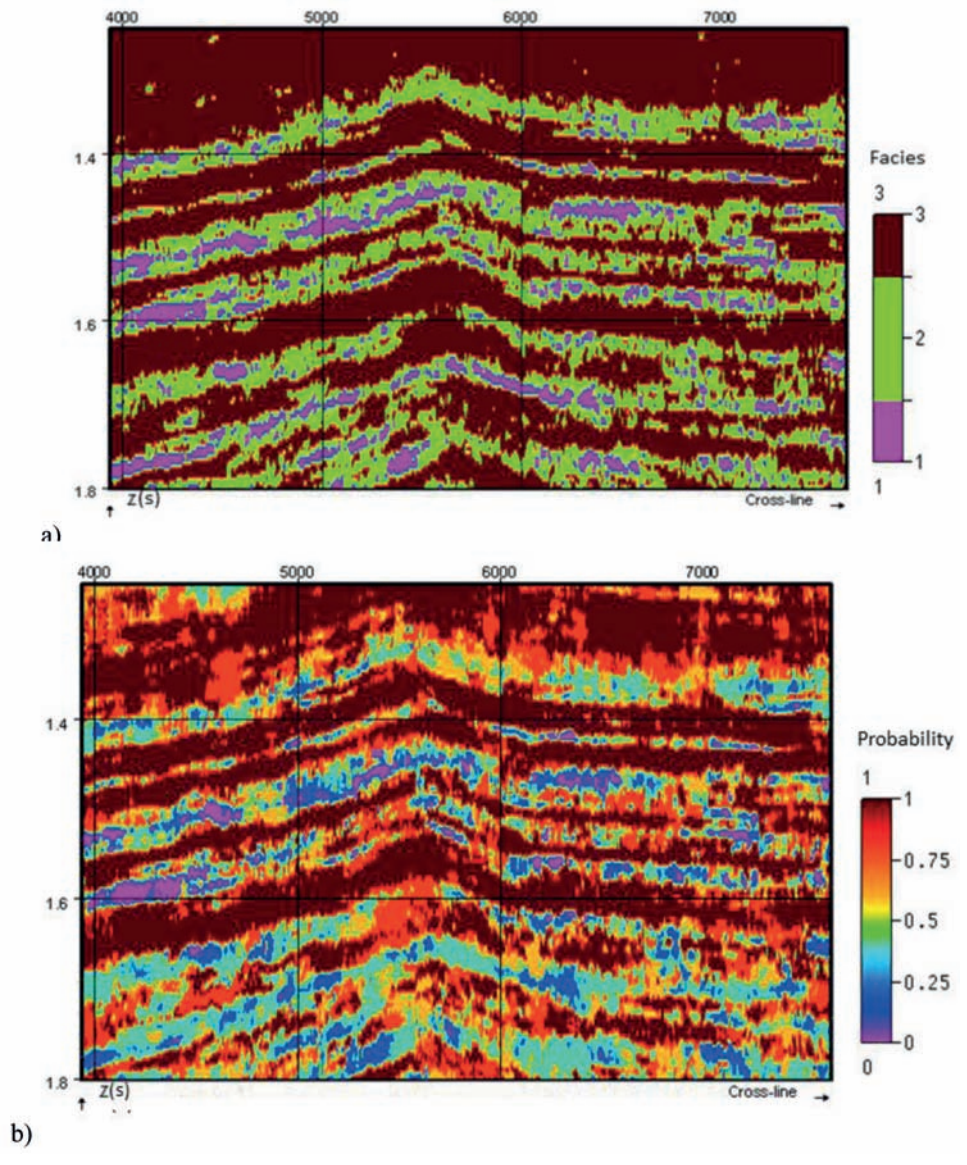

Fig. 14. (a) Facies clustering at well A location (inline 1100) with probability more than 0.8 for facies 3. (b) Probability section for facies 3.

CONCLUSIONS

In this study, a carbonate gas field of Iran was studied for probabilistic forecasting of facies distribution. Stochastic inversion based on spectral simulation was used to obtain acoustic impedance attribute and add low frequency component to AI model. Some conclusions were obtained as follows:

1. Comparison between stochastic and deterministic inversion method showed that the former provided lower error than the latter.

2. Standard deviation of the realizations showed that variability was much larger than the case with there was relatively slight well constraint on the model. Therefore, accuracy of the model was proportional to well constraints.

3. Evaluation of the neural network classification illustrated that there were three facies in this study: favorable, unfavorable, and moderate for reservoir qualities. The results were correlated by porosity and checked by litho-stratigraphic chart, which showed good correlation. It can be concluded that the AI was a good parameter for facies estimation in this case study.

4. The connectivity algorithm has a simple structure to obtain probability facies cube when there is multiple realization of a problem. Final results represented that unfavorable zones were thin beds and favorable zones were massive layers with high probability.

5. The methodology applied in this paper was able to estimate high probable facies from the large volume 3D seismic data. Therefore, exploration success rate can increase in petroleum industries using proposed method.

ACKNOWLEDGMENTS

The authors acknowledge the R&D of the National Iranian Oil Company (NIOC) and Pars Oil and Gas Company (POGC) for providing the data and permission to publish this paper.

REFERENCES

Bortoli, L.J., Alabert, F., Haas, A. and Journel, A., 1993. Constraining stochastic images to seismic data. In: Soares, A. (Ed.), Quantitative Geology and Geostatistics: Geostatistics Troia 92. Springer Verlag, Dordrecht, p. 325-337.

Bosch, M., Mukerji, T. and Gonzalez, E.F., 2010. Seismic inversion for reservoir properties combining statistical rock physics and geostatistics - a review. Geophysics, 75(5): 165-76.

Buland, A. and Omre, H., 2003. Bayesian linearized AVO inversion. Geophysics, 68: 185-198.
Cooke, D.A. and Schneider, W.A., 1983. Generalized linear inversion of reflection seismic data. Geophysics, 48: 665-676.
Debeye, H.W.J., Sabbah, E. and van der Made, P.M., 1996. Stochastic inversion. Expanding Abstr., 66th Ann. Internat. SEG Mtg., Denver: 1212-1215.
Deutsch, C., 1998. FORTRAN programs for calculating connectivity of three dimensional numerical models and for ranking multiple realizations. Comput. Geosci., 24: 69-76.
Deutsch, C. and Journel, A., 1998. GSLIB - Geostatistical Software Library and User's Guide. Oxford University Press, New York.
Eidsvik, J., Avseth, P., More, H., Mukerji, T. and Mavko, G., 2004. Stochastic reservoir characterization using prestack seismic data. Geophysics, 69: 978-993.
Francis, A., 2005. Limitations of deterministic and advantages of stochastic seismic inversion. CSEG Recorder, 30(2): 5-11.
Francis, A., 2006a. Understanding stochastic inversion - Part 1. First break, 24(11): 69-77.
Francis, A., 2006b. Understanding stochastic inversion - Part 2. First break, 24 (12): 79-84.
Gersho, A. and Gray, R.M., 1992. Vector Quantization and Signal Compression. Kluwer Academic Publishers, New York.
Gonzalez, E.F., Mukerji, T. and Mavko., G., 2008. Seismic inversion combining rock physics and multiple-point geostatistics. Geophysics, 73(1): R11-R21.
Haas, A. and Dubrule, O., 1994. Geostatical inversion: a sequential method of stochastic reservoir modeling constrained by seismic data. First break, 12: 561-569.
Kane, J., Rodi, W., Herrmann, F. and Toksöz, M.N., 1999. Geostatistical seismic inversion using well log constraints. Expanding Abstr., 69th Ann. Internat. SEG Mtg., Houston: 1504-1507.
Kelkar, M. and Perez, G., 2002. Applied Geostatistics for Reservoir Characterization. Soc. Petrol. Engin. Publicat., Richardson, TX: 52-97.
Lancaster, S. and Whitcombe, D., 2000. Fast-track coloured inversion. Expanding Abstr., 70th Ann. Internat. SEG Mtg., Calgary, AB: 1572-1575.
Matos, M.C., Osório, P.L.M. and Johann, P.R.S., 2005. Vertical seismic facies detection through unsupervised 3D voxel based seismic facies classification applied to a turbidite field in Campose Basin - Brazil. 9th Internat. Congr. Braz. Geophys. Soc., Salvador, Brazil.
Pardo-Iguzquiza, E. and Chica-Olmo, M., 1993. The Fourier integral method - an efficient spectral method for simulation of random fields. Mathemat. Geol., 25: 177-217.
Russel, B., 1988. Model-based Inversion. Introduction to Seismic Inversion Methods. SEG, Tulsa, OK.
Russel, B., 2005. Neural network applications in geophysics. CSEG Nat. Conv.: 339-342.
Tavakoli, V., Rahimpour-Bonab, H. and Esrafili-Dizaji, B., 2011. Diagenetic controlled reservoir quality of South Pars gas field - an integrated approach. Comptes Rendus Geosc., 343: 55-71.
Taner, M.T., Schuelke, J.S., O'Doherty, R. and Baysal, E., 1994. Seismic attributes revisited. Expanded Abstr., 64th Ann. Internat. SEG Mtg., Los Angeles: 1104-1106.
Yao, T., Calvert, C., Bishop, G., Jones, T., Ma, Y. and Foreman, L., 2004. Spectral component geologic modeling - a new technology for integrating seismic information at the correct scale. In: Leuangthong, O. and Deutsch, C.V. (Eds.), Geostatistics Banff. Springer Verlag, Dordrecht: 23-33.